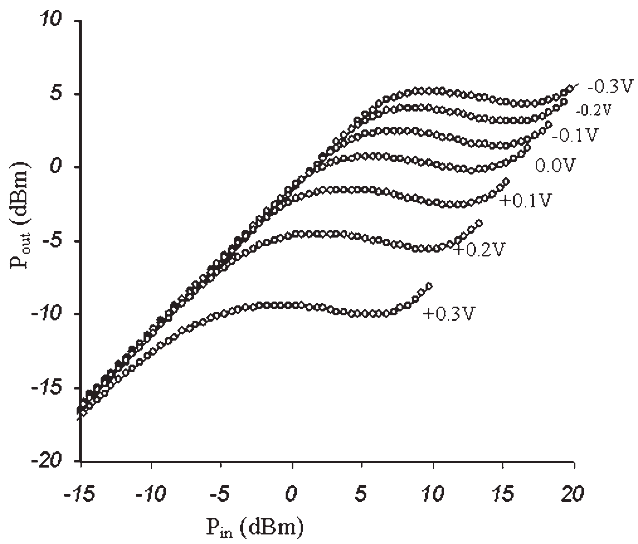

Figure 6 Tested P_{in} Vs P_{out} of the limiter at different control voltages

c. Attenuation decreases with the increase of RF power level for control voltage more than 0.4 V.

For limiter function, attenuation should increase with the increase of RF power level. Therefore, for the limiter circuit using these Schottky diodes, the control voltage should be <0.4 V.

Figure 5 shows the tested output power (P_{out}) with input power (P_{in}) of the limiter circuit at control voltage (V_c) of 0 V for different values of bias resistor (R_b). The tested insertion loss of the assembled limiter is nearly 0.9 dB at small signal condition at all values of bias resistor. The deep of the I–O curves are correspond to the diode impedance of 50 Ω, here the circuit provides maximum attenuation. The plot shows that rate of change of attenuation with the input RF power level is a function of bias resistor (R_b). This is also evident from the bias load lines L1 and L3 in Figure 1 corresponds to same supply voltage but with higher and lower value of bias resistors, respectively. In case of L3, RF resistance of the diodes decreases sharply than in case of L1 with the increase of RF power level. It is also clear from the plot that to keep output power nearly constant, over the limiting power level, there is an optimum bias resistor. In this case it is nearly 10 Ω. In case of 10 Ω bias resistor, the flat leakage is nearly within 1.5 dB around output power of 0-dBm over the input power range of 15 dB.

Figure 6 shows the input-output characteristic of the limiter at bias resistor of 10 Ω for different values of V_c. The plot shows that by changing V_c, limiting power level can be adjusted. It shows that with the variation of control voltage from −0.3 to +0.3 V, limiting power level varies from −10 to +5 dBm. For each control voltage, the limiting power range is nearly 15 dB. Beyond the limiting power range, increases of output power levels are because of the decrease of diode impedance beyond 50 Ω. Another important observation is that for all values of control voltages up to 0.2 V, I–O curves are very much linear at small signal condition. However, for control voltage = 0.3 V, small signal insertion loss increases thus introduces some nonlinearity in the I–O curves.

5. CONCLUSION

The article presents the nonlinear behavior of Schottky diodes under different bias load line conditions and discusses the suitable bias conditions for using the Schottky diodes as limiter. This article presents design and test results of a Schottky barrier diode limiter at microwave frequency. The test result shows that the Schottky diode limiter circuit provides nearly 1.5 dB flat leakage over the input power level of 15 dB. It is also demonstrated upto 15 dB range of threshold power level adjustment. The adjustability of the threshold power level by bias adjustment will eliminate the optimization of diode structure for limiting of different power levels.

REFERENCES

1. K. Miyazaki, T. Ohata, T. Ono, A. Kamikokura, R. Hayashi, K. Seino, H. Hirose, and H. Kurebayashi, L-band 50W SSPA incorporating overdrive limitation circuit and power saving circuit for MTSAT, 17th International Communications Satellite Systems Conference and Exhibit, Yokohama, Japan, 1998, pp. 23–27.
2. S.C. Bera and R.V. Singh, A temperature-compensated closed loop overdrive level controller for microwave solid-state power amplifiers, Microwave J 47 (2004), 114–122.
3. S.S. Yang, T.Y. Kim, D.K. Kong, S.S. Kim, and K.W. Yeom, A novel analysis of a Ku-band planar p-i-n diode limiter, IEEE Trans Microwave Theory Tech 57 (2009), 1447–1460.
4. D.G. Smith, D.D. Heston, J. Heston, B. Heimer, and K. Decker, Designing high-power limiter circuit with GaAs PIN diodes, IEEE MTT-S Int Microwave Symp Dig, Orlando, FL (1979), 329–331.
5. J. Erikson, N. Rorsman, and H. Zirath, Microwave silicon carbide Schottky diodes, Electron Lett 37 (2001), 250–252.
6. J. Erikson, N. Rorsman, and H. Zirath, 4H-silicon carbide Schottky barrier diodes for microwave applications, IEEE Trans Microwave Theory Tech 51 (2003), 796–804.
7. M. Sudow, K. Andersson, N. Billstrom, J. Grahn, H. Hjelmgren, J. Nilsson, P.A. Nilsson, J. Stahl, H. Zirath, and N. Rorsman, An SiC MESFET-Based MMIC Process, IEEE Trans Microwave Theory Tech 54 (2006), 4072–4078.
8. S.M. Sze, Physics of semiconductor devices, 2nd ed., Wiley-Interscience, New York, 1982.

INTERNAL PRINTED LOOP/MONOPOLE COMBO ANTENNA FOR LTE/GSM/UMTS OPERATION IN THE LAPTOP COMPUTER

Ting-Wei Kang and Kin-Lu Wong
Department of Electrical Engineering, National Sun Yat-Sen University, Kaohsiung 80424, Taiwan; Corresponding author: kangtw@ema.ee.nsysu.edu.tw

Received 24 September 2009

ABSTRACT: *A promising internal laptop computer antenna capable of generating two wide operating bands to respectively cover the LTE700/GSM850/900 (698∼960 MHz) and GSM1800/1900/UMTS/LTE2300/2500 (1710∼2690 MHz) operation is presented. The antenna occupies a size of 85 × 10 × 4 mm³ along the top edge of the supporting metal frame of the display panel and is suitable to be embedded inside the casing of the laptop computer for practical applications. The antenna is a printed loop/monopole combo antenna formed by combining a quarter-wavelength printed loop with an internal matching circuit and a printed monopole with an internal distributed inductor. The proposed combo antenna leads to reduced size yet wide bandwidth to cover the eight-band LTE/GSM/UMTS operation.* © 2010 Wiley Periodicals, Inc. Microwave Opt Technol Lett 52: 1673–1678, 2010; Published online in Wiley InterScience (www.interscience.wiley.com). DOI 10.1002/mop.25256

Key words: *mobile antennas; internal laptop computer antennas; printed loop antennas; printed monopole antennas; combo antennas*

1. INTRODUCTION

As the long term evolution (LTE) service [1] can provide better mobile broadband and multimedia services than the existing GSM and UMTS mobile networks [2], it has recently become attractive to incorporate the LTE with the GSM/UMTS operation in the mobile devices. For this application, however, there are very few of the internal mobile device antennas providing the required bandwidths in covering all the operating bands of the LTE/GSM/UMTS operation; they include three LTE bands in the LTE700 (698∼787 MHz), LTE2300 (2305∼2400 MHz), and LTE2500 (2500∼2690 MHz), four GSM bands in the GSM850 (824∼894 MHz), GSM900 (880∼960 MHz), GSM1800 (1710∼1880 MHz), and GSM1900 (1850∼1990 MHz), and one UMTS band (1920∼2170 MHz). That is, an eight-band internal mobile device antenna for the LTE/GSM/UMTS operation is required. This imposes a challenge for the internal antenna design, as there is usually very limited space offered in the mobile device for the embedded internal antennas. The available internal laptop computer antennas that have been reported in the published papers are mainly for covering the five-band GSM850/900/1800/1900/UMTS operation [3–10]. To our knowledge, at present, there are no reported internal laptop computer antennas satisfying the eight-band LTE/GSM/UMTS operation.

In this article, we present a promising internal laptop computer antenna of small size 85 × 10 × 4 mm^3 to generate two wide operating bands to respectively cover the LTE700/GSM850/900 (698∼960 MHz) and GSM1800/1900/UMTS/LTE2300/2500 (1710∼2690 MHz) operation. The small occupied size allows the antenna to be embedded in the laptop computer as an internal antenna. The antenna is a printed loop/monopole combo antenna, which is formed by combining a quarter-wavelength printed loop with an internal matching circuit [11, 12] and a printed monopole with an internal distributed inductor [13, 14] into one antenna. The proposed combo antenna leads to reduced size yet wide bandwidth for the antenna to cover the eight-band LTE/GSM/UMTS operation. Details of the proposed combo antenna are studied in the article, and the results of the fabricated prototype are presented and discussed.

2. PROPOSED PRINTED LOOP/MONOPOLE COMBO ANTENNA

Figure 1 shows the geometry of the proposed printed loop/monopole combo antenna for LTE/GSM/UMTS operation in the laptop computer. The antenna is mounted along the top edge of the supporting metal frame (a 0.2-mm thick copper plate measuring 220 × 260 mm^2 in this study) of the display panel. By considering the practical practice that the central region of the top edge of the display panel is usually reserved for the lens of the embedded camera in the modern laptop computers, the proposed antenna is placed along the top edge with a spacing of 30 mm to the central line. The antenna has a length of 85 mm along the top edge (y direction), a height of 10 mm above the top edge (z direction), and a thickness of 4 mm in the x direction.

The antenna is mainly formed by using a printed loop with an internal matching circuit and a printed monopole with an internal distributed inductor. In addition to the major portions of the loop and monopole printed on a 0.4-mm thick FR4 substrate, the widened end portion of size 3.6 × 40 mm^2 for the monopole and the widened central portion of size 3.6 × 36 mm^2 for the loop are added, which help achieve widened bandwidths in

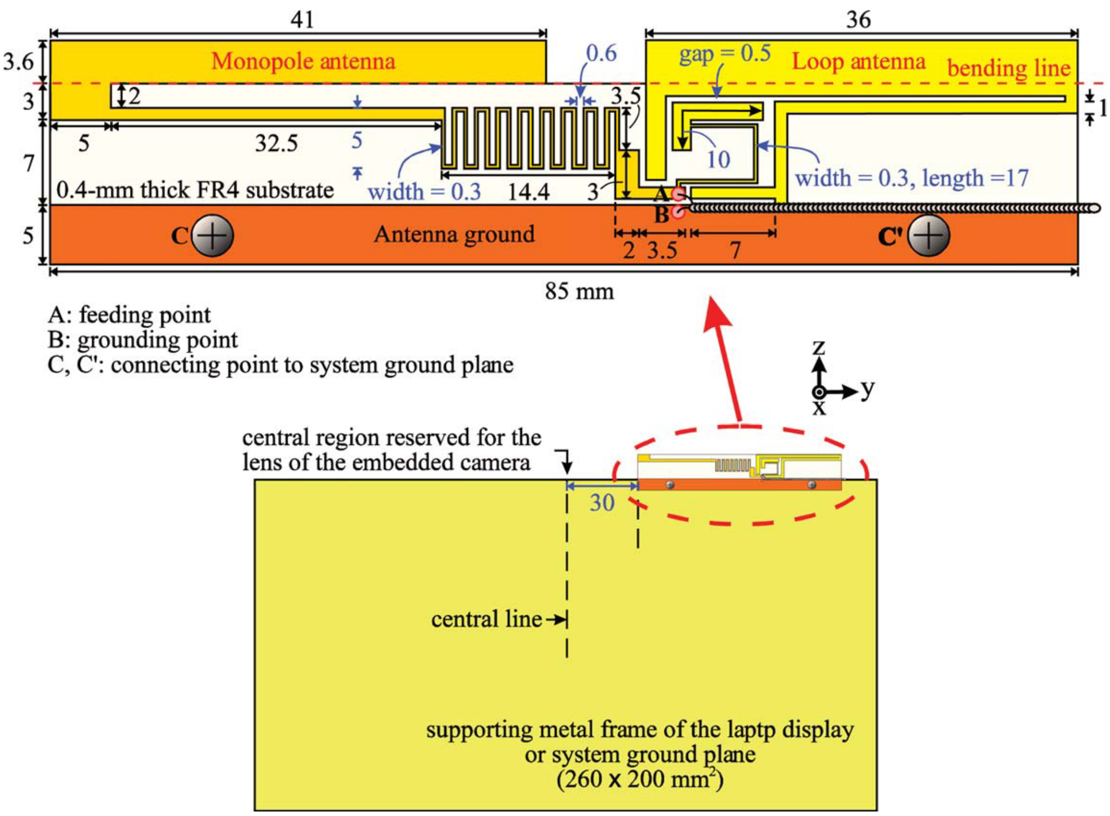

Figure 1 Geometry of the proposed printed loop/monopole combo antenna mounted along the top edge of the supporting metal frame of the display panel in the laptop computer for LTE/GSM/UMTS operation. [Color figure can be viewed in the online issue, which is available at www.interscience.wiley.com]

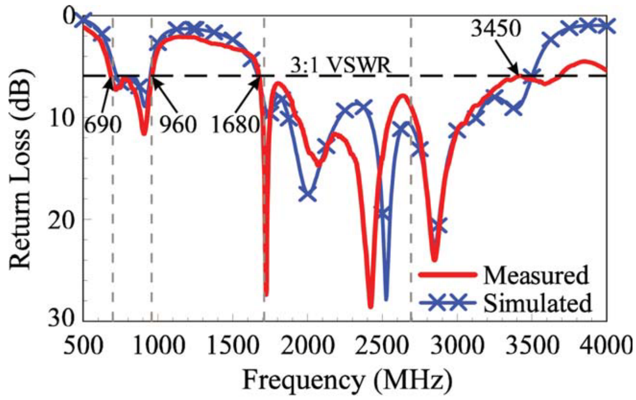

(a)

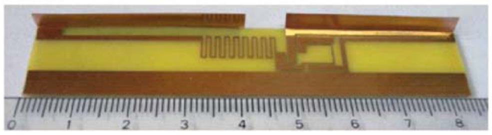

photo of fabricated prototype

(b)

Figure 2 (a) Measured and simulated return loss for the proposed antenna. (b) Photo of the fabricated prototype. [Color figure can be viewed in the online issue, which is available at www.interscience.wiley.com]

the lower and upper bands of the proposed antenna. The two widened portions are cut from a 0.2-mm thick copper plate and are aligned to be in the *x-y* plane, orthogonal to the supporting metal frame in the *y-z* plane. In this case, with the inclusion of the 0.4-mm thick FR4 substrate, the thickness of the proposed antenna in the *x* direction is 4 mm only, which is acceptable to be embedded inside the casing of the laptop computer. The printed loop and monopole share a common feeding point A and a common grounding point B at the antenna ground (size 5×85 mm^2, also printed on the 0.4-mm thick FR4 substrate); both point A and B are, respectively, connected to the central conductor and outer grounding sheath of a 50-Ω mini coaxial line for testing the antenna in the experiment. The antenna ground is electrically connected to the supporting metal frame of the laptop display through two via-holes at point C and C′ shown in the figure.

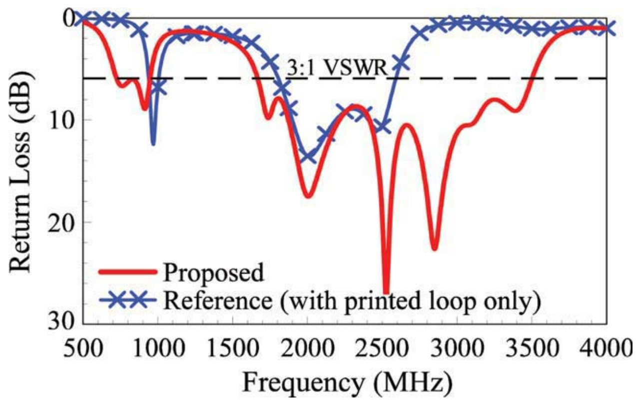

Figure 3 Simulated return loss for the proposed antenna and the case with the printed loop only. [Color figure can be viewed in the online issue, which is available at www.interscience.wiley.com]

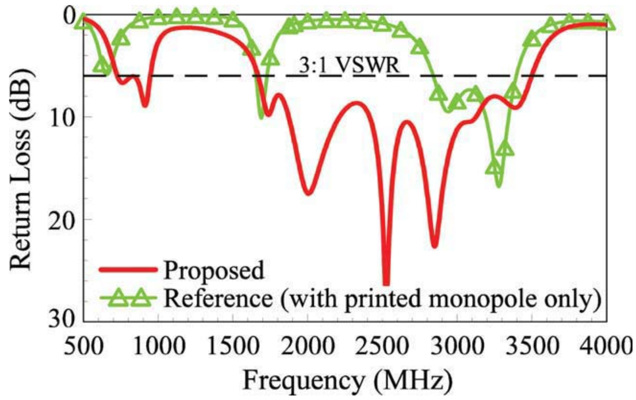

Figure 4 Simulated return loss for the proposed antenna and the case with the printed monopole only. [Color figure can be viewed in the online issue, which is available at www.interscience.wiley.com]

In the printed loop, the internal matching circuit consisting of a coupling strip and an inductive strip is equivalent to a series LC matching circuit [11, 12]. The inductive strip of width 0.3 mm functions as an inductive element and its length is selected to be 17 mm in this study. The coupling strip is tuned to have a length of 10 mm, which is capacitively coupled to the front portion of the printed loop through a coupling gap of 0.5 mm; this provides capacitive reactance and functions as a series capacitive element. With the proper internal matching circuit selected, the printed loop can be excited at its quarter-wavelength resonant mode at about 900 MHz [11] for size reduction, which is different from the half-wavelength mode excitation of many traditional loop antennas for mobile phone applications [15–30].

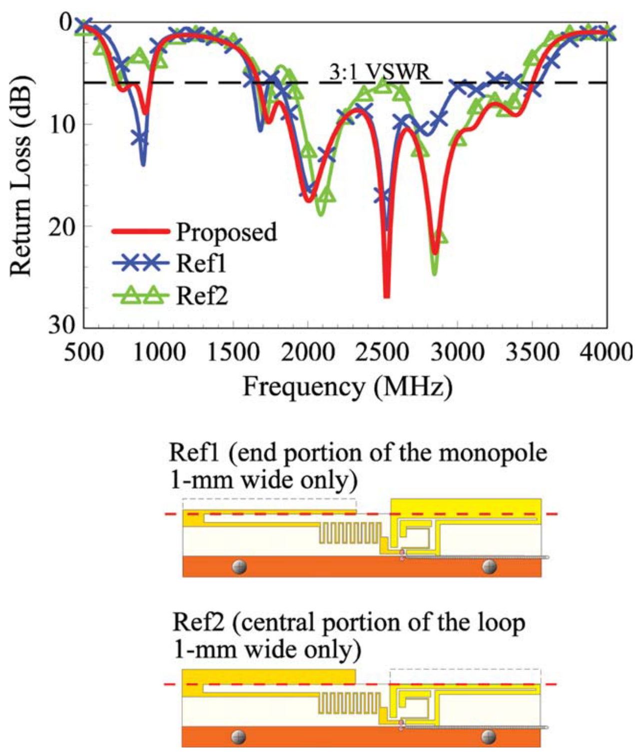

Figure 5 Simulated return loss for the proposed antenna, the case with 1-mm wide end portion in the printed monopole (Ref. 1), and the case with 1-mm wide central portion in the printed loop (Ref. 2). [Color figure can be viewed in the online issue, which is available at www.interscience.wiley.com]

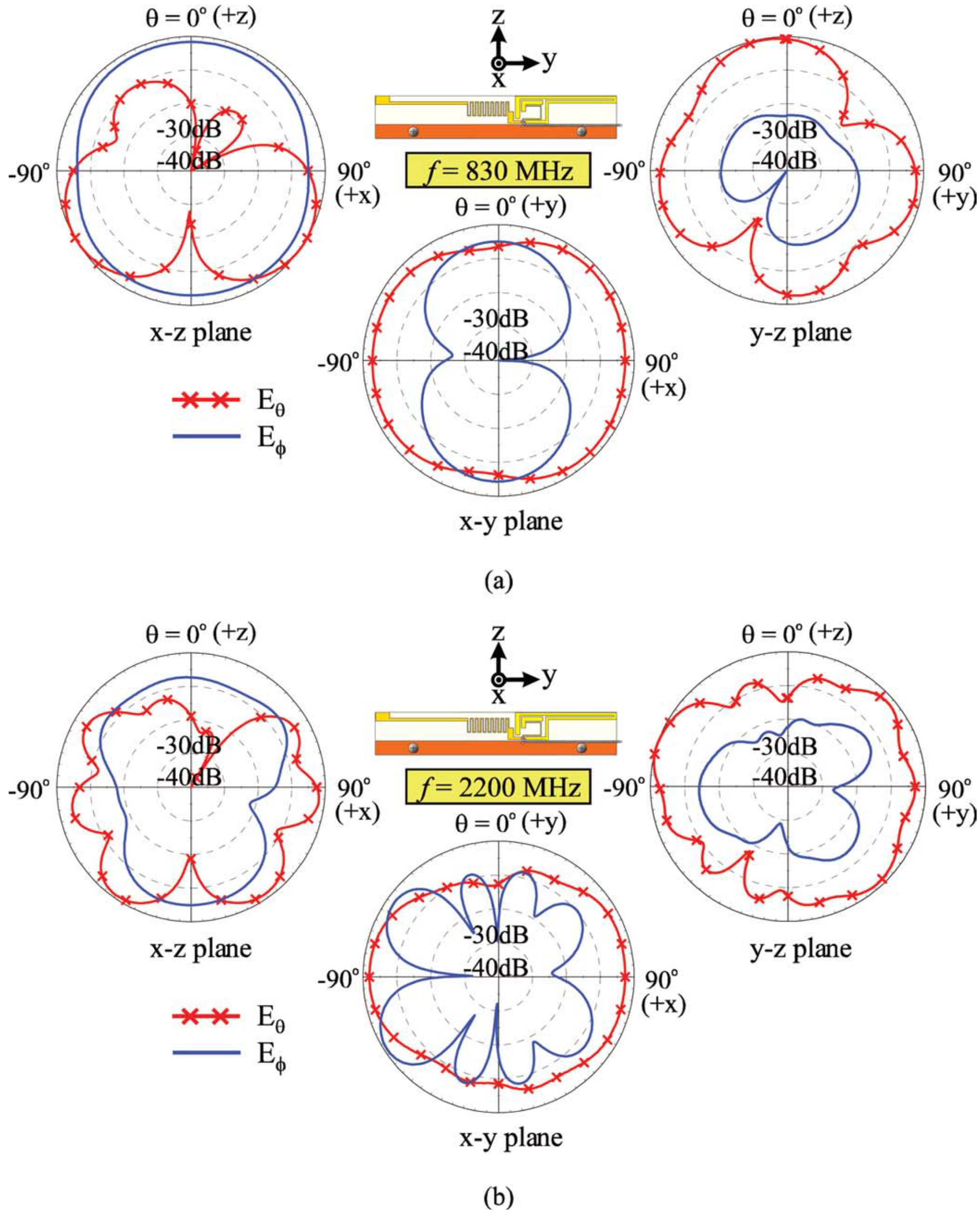

Figure 6 Measured radiation patterns at (a) 830 MHz and (b) 2200 MHz for the proposed antenna. [Color figure can be viewed in the online issue, which is available at www.interscience.wiley.com]

The internal matching circuit can also lead to bandwidth widening of the higher-order modes of the printed loop. Detailed operating principle of the quarter-wavelength printed loop with the internal matching circuit has been presented in [11]. However, with the printed loop only, the obtained bandwidths of the antenna's lower and upper bands are still not wide enough for covering the desired eight-band LTE/GSM/UMTS operation, especially the lower-band bandwidth far from covering the LTE700/GSM850/900 operation in the 698∼960 MHz band.

To achieve a wide lower band to cover the LTE700/GSM850/900 operation, the printed monopole is added in the proposed antenna. To achieve a reduced-size printed monopole, a meandered section (line width 0.3 mm, line spacing 0.6 mm) is introduced in the front portion of the monopole. This meandered section functions as a distributed inductor that contributes additional inductance to compensate for the increased capacitance resulting from the decreased resonant length of the monopole [14, 31, 32]. Effects of the distributed inductor on reducing the resonant length of the printed monopole have also been shown in [14]. With the distributor inductor and the widened end portion, the printed monopole provides a resonant mode at about 750 MHz to incorporate the quarter-wavelength loop mode at about 900 MHz to achieve a wide lower band for the LTE/GSM850/900 operation. In addition, the printed monopole also contributes its higher-order resonant modes to incorporate those generated by the printed loop to achieve a wide upper band to cover the desired LTE1800/1900/UMTS/LTE2300/2500 operation in the 1710∼2690 MHz band.

3. RESULTS AND DISCUSSION

The proposed antenna was fabricated and measured. Figure 2(a) shows the measured and simulated return loss of the fabricated prototype; the photo of the fabricated prototype is also shown in Figure 2(b). The simulated results obtained using Ansoft HFSS

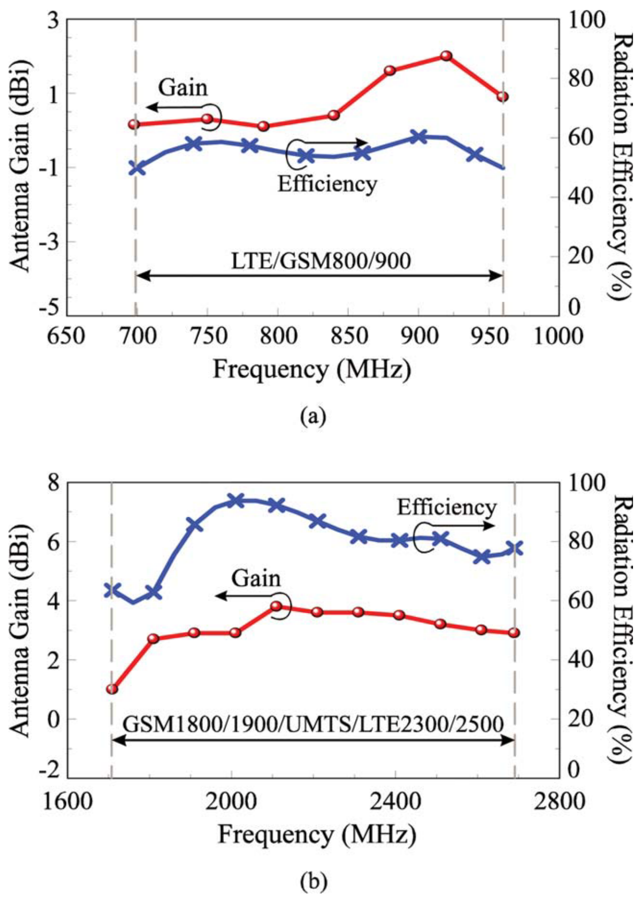

Figure 7 Measured antenna gain and simulated radiation efficiency for the proposed antenna. (a) The lower band (698∼960 MHz). (b) The upper band (1710∼2690 MHz). [Color figure can be viewed in the online issue, which is available at www.interscience.wiley.com]

[33] are seen to agree with measured data. Two wide operating bands are obtained. The measured 3:1 VSWR bandwidth of the lower band reaches 270 MHz (690∼960 MHz), which covers the LTE700/GSM850/900 operation in the 698∼960 MHz. The upper-band bandwidth is larger than 1.7 GHz (1680∼3450 MHz) and covers the LTE1800/1900/UMTS/LTE2300/2500 operation in the 1710∼2690 MHz band. Notice that the 3:1 VSWR bandwidth definition is widely used in the internal mobile device antenna for WWAN (wireless wide area network) operation.

Figure 3 shows the simulated return loss for the proposed antenna and the case with the printed loop only. Without the presence of the printed monopole, the antenna's lower band is narrow in bandwidth and far from covering the desired operating bands. From the results, it can be seen that a resonant mode at about 750 MHz is generated by the adding of the printed monopole in the proposed antenna, and the resonant mode at about 900 MHz contributed by the printed loop is also widened. The two resonant modes together form the wide lower band for the proposed antenna. Also, owing to the adding of the printed monopole, which contributes its higher-order modes, the impedance matching for frequencies around 1700 MHz and those higher than about 2500 MHz is improved, resulting in a much widened bandwidth for the antenna's upper band.

Figure 4 shows the simulated return loss for the proposed antenna and the case with the printed monopole only. A first or lowest resonant mode contributed to the antenna's lower band, a second mode at about 1700 MHz, and a third dual-resonant mode at about 3000 MHz are seen. The second and third modes contributed to the antenna's upper band to achieve a very wide bandwidth of larger than 1.7 GHz in this study.

Figure 5 shows a comparison of the simulated return loss for the proposed antenna, the case with 1-mm wide end portion in the printed monopole (Ref. 1), and the case with 1-mm wide central portion in the printed loop (Ref. 2) is shown in the figure. Results clearly indicate that the two widened portions are crucial in achieving good impedance matching of the two resonant modes in the antenna's lower band, and the impedance matching improvement for frequencies over the antenna's upper band is also obtained as well.

Figure 6 plots the measured radiation patterns at 830 and 2200 MHz (central frequencies of the 698∼960 and 1710∼2690 MHz bands) for the proposed antenna. In the *x-y* plane, the vertical radiation E_θ at both frequencies is near-omnidirectional, which is advantageous for practical applications to achieve good coverage in all the directions in the azimuthal plane. Figure 7 presents the measured antenna gain and simulated radiation efficiency for the proposed antenna. Results for the desired lower band are shown in Figure 7(a), while those for the desired upper band are shown in Figure 7(b). The measured antenna gain is about 0∼2.0 dBi over the 698∼960 MHz band, and 1.0∼3.7 dBi over the 1710∼2690 MHz band. For the simulated radiation efficiency, which includes the mismatch loss, it is about 50∼60% and 60∼90% over the 698∼960 MHz and 1710∼2690 MHz, respectively.

Also, note that the 3D average antenna gain defined as the antenna gain over all of the space [28] is another important radiation characteristic to be considered for practical laptop computer applications. The 3D average antenna gain has been derived to be equivalent to the radiation efficiency of the antenna

TABLE 1 Simulated 3D Average Antenna Gain for the Proposed Antenna

Average Antenna Gain (dBi)		Proposed Antenna (dBi)	Proposed Antenna with 70-cm Mini Coaxial Line Loss (dBi)	Specification (dBi)
The Lower Band: (Tx for Transmitting and Rx for Receiving)				
LTE700 band	728 MHz (Tx)	−2.5	−3.5	−3.5
	757 MHz (Rx)	−2.3	−3.3	−3.5
GSM850 band	836 MHz (Tx)	−2.3	−3.3	−3.3
	880 MHz (Rx)	−2.4	−3.4	−4.0
GSM900 band	900 MHz (Tx)	−2.2	−3.2	−4.0
	940 MHz (Rx)	−2.6	−3.6	−6.0
The Upper Band: (Tx for Transmitting and Rx for Receiving)				
GSM1800 band	1750 MHz (Tx)	−2.0	−4.0	−4.0
	1840 MHz (Rx)	−1.5	−3.5	−6.0
GSM1900 band	1880 MHz (Tx)	−1.0	−3.0	−3.3
	1960 MHz (Rx)	−0.4	−2.4	−4.5
UMTS band	1950 MHz (Tx)	−0.4	−2.4	−4.5
	2140 MHz (Rx)	−0.4	−2.4	−6.0
LTE2300 band	2345 MHz (Tx/Rx)	−0.9	−2.9	−3.5
LTE2500 band	2535 MHz (Tx)	−1.0	−3.0	−3.5
	2655 MHz (Rx)	−1.2	−3.2	−6.0

The specification is the minimum average antenna gain required for practical applications of the internal antenna in the laptop computers [7]. The loss owing to the 70-cm mini coaxial line used in practical laptop computers is estimated to be −1 dB in the lower band and −2 dB in the upper band.

[28], whose minimum values acceptable for practical applications in the LTE/GSM/UMTS bands are listed in Table 1 as the specification. As in the practical cases the internal antennas embedded at the top edge of the laptop display usually include a long mini coaxial line of about 70 cm to connect the antennas to the RF module at the base of the laptop computer, the power loss associated with the mini coaxial line should be considered to meet the specification listed in Table 1. It is reasonable to estimate that the power loss owing to the 70-cm mini coaxial line is about -1 dB in the lower band and about -2 dB in the upper band [28]. The results given in the table indicate that the 3D average antenna gain of the proposed antenna meets the required specification over the eight-band LTE/GSM/UMTS bands.

4. CONCLUSIONS

A combo antenna formed by a printed monopole and a printed loop suitable for eight-band LTE/GSM/UMTS operation in the laptop computer has been proposed. The antenna has been fabricated and tested. It has been shown that the printed monopole and the printed loop can be, respectively, adjusted such that their contributed resonant modes are incorporated into two wide operating bands for the proposed antenna. The wide lower band covers the 698$\sim$960 MHz band for the LTE700/GSM850/900 operation, whereas the wide upper band covers the 1710$\sim$2690 MHz for the GSM1800/1900/UMTS/LTE2300/2500 operation. The antenna also shows good radiation performances over the eight operating bands. Further, the antenna occupies a size of $85 \times 10 \times 4$ mm^3 when mounted along the top edge of the laptop display, making it promising to be applied as an internal laptop computer antenna.

REFERENCES

1. S. Sesia, I. Toufik, and M. Baker (Eds), LTE, The UMTS Long Term Evolution, From Theory to Practice, Wiley, New York, 2009.
2. K.L. Wong, Planar Antennas for Wireless Communications, Wiley, New York, 2003.
3. X. Wang, W. Chen, and Z. Feng, Multiband antenna with parasitic branches for laptop applications, Electron Lett 43 (2007), 1012–1013.
4. C.H. Chang and K.L. Wong, Internal coupled-fed shorted monopole antenna for GSM850/900/1800/1900/UMTS operation in the laptop computer, IEEE Trans Antennas Propag 56 (2008), 3600–3604.
5. C. Zhang, S. Yang, S. El-Ghazaly, A.E. Fathy, and V.K. Nair, A low-profile branched monopole laptop reconfigurable multiband antenna for wireless applications, IEEE Antennas Wireless Propag Lett 8 (2009), 216–219.
6. K.L. Wong and S.J. Liao, Uniplanar coupled-fed printed PIFA for WWAN operation in the laptop computer, Microw Opt Technol Lett 51 (2009), 549–554.
7. K.L. Wong and L.C. Lee, Multiband printed monopole slot antenna for WWAN operation in the laptop computer, IEEE Trans Antennas Propag 57 (2009), 324–330.
8. K.L. Wong and F.H. Chu, Internal planar WWAN laptop computer antenna using monopole slot elements, Microw Opt Technol Lett 51 (2009), 1274–1279.
9. C.W. Chiu, Y.J. Chi, and S.M. Deng, An internal multiband antenna for WLAN and WWAN applications, Microw Opt Technol Lett 51 (2009), 1803–1807.
10. C.T. Lee and K.L. Wong, Study of a uniplanar printed internal WWAN laptop computer antenna including user's hand effects, Microwave Opt Technol Lett 51 (2009), 2341–2346.
11. Y.W. Chi and K.L. Wong, Quarter-wavelength printed loop antenna with an internal printed matching circuit for GSM/DCS/PCS/UMTS operation in the mobile phone, IEEE Trans Antennas Propag 57 (2009), 2541–2547.
12. Y.W. Chi and K.L. Wong, Very-small-size printed loop antenna for GSM/DCS/ PCS/UMTS operation in the mobile phone, Microw Opt Technol Lett 51 (2009), 184–192.
13. T.W. Kang and K.L. Wong, Chip-inductor-embedded small-size printed strip monopole for WWAN operation in the mobile phone, Microw Opt Technol Lett 51 (2009), 966–971.
14. C.H. Chang and K.L. Wong, Small-size printed monopole with a printed distributed inductor for penta-band WWAN mobile phone application, Microw Opt Technol Lett 51 (2009), 2903–2908.
15. C.A. Balanis, K.D. Katsiba, P.A. Tirkas, and C.R. Birtcher, Loop antenna for mobile and personal communication systems, 1997 IEEE Vehicular Technol Conf 2 (1997), 452–454.
16. T. Adachi, A. Hirata, and T. Shiozawa, Folded-loop antennas for handset terminals at the 2.0-GHz band, Microw Opt Technol Lett 36 (2003), 376–378.
17. B.K. Yu, B. Jung, H.J. Lee, F.J. Harackiewicz, and B. Lee, A folded and bent internal loop antenna for GSM/DCS/PCS operation of mobile handset applications, Microw Opt Technol Lett 48 (2006), 463–467.
18. B. Jung, H. Rhyu, Y.J. Lee, F.J. Harackiewicz, M.J. Park, and B. Lee, Internal folded loop antenna with tuning notches for GSM/GPS/DCS/PCS mobile handset applications, Microw Opt Technol Lett 48 (2006), 1501–1504.
19. Y.W. Chi and K.L. Wong, Internal compact dual-band printed loop antenna for mobile phone application, IEEE Trans Antennas Propag 55 (2007), 1457–1462.
20. C.I. Lin and K.L. Wong, Internal meandered loop antenna for GSM/DCS/PCS multiband operation in a mobile phone with the user's hand, Microw Opt Technol Lett 49 (2007), 759–765.
21. W.Y. Li and K.L. Wong, Surface-mount loop antenna for AMPS/GSM/DCS/PCS operation in the PDA phone, Microw Opt Technol Lett 49 (2007), 2250–2254.
22. W.Y. Li and K.L. Wong, Internal printed loop-type mobile phone antenna for penta-band operation, Microw Opt Technol Lett 49 (2007), 2595–2599.
23. C.I. Lin and K.L. Wong, Internal multiband loop antenna for GSM/DCS/PCS/UMTS operation in the small-size mobile phone, Microw Opt Technol Lett 50 (2008), 1279–1285.
24. K.L. Wong and C.H. Huang, Printed loop antenna with a perpendicular feed for penta-band mobile phone application, IEEE Trans Antennas Propag 56 (2008), 2138–2141.
25. Y.W. Chi and K.L. Wong, Half-wavelength loop strip fed by a printed monopole for penta-band mobile phone antenna, Microw Opt Technol Lett 50 (2008), 2549–2554.
26. K.L. Wong and S.Y. Tu, Ultra-wideband coupled-fed loop antenna for penta-band folder-type mobile phone, Microw Opt Technol Lett 50 (2008), 2706–2712.
27. Y.W. Chi and K.L. Wong, Compact multiband folded loop chip antenna for small-size mobile phone, IEEE Trans Antennas Propag 56 (2008), 3797–3803.
28. W.Y. Li and K.L. Wong, Seven-band surface-mount loop antenna with a capacitively coupled feed for mobile phone application, Microw Opt Technol Lett 51 (2009), 81–88.
29. Y.W. Chi and K.L. Wong, Very-small-size folded loop antenna with a band-stop matching circuit for WWAN operation in the mobile phone, Microw Opt Technol Lett 51 (2009), 808–814.
30. K.L. Wong and W.Y. Chen, Small-size printed loop antenna for penta-band thin-profile mobile phone application, Microw Opt Technol Lett 51 (2009), 1512–1517.
31. J. Carr, Antenna Toolkit, 2nd ed., Newnes, Oxford, U.K., 2001, pp. 111–112.
32. J. Thaysen and K.B. Jakobsen, A size reduction technique for mobile phone PIFA antennas using lumped inductors, Microw J 48 (2005), 114–126.
33. Ansoft Corporation, Available at: http://www.ansoft.com/products/hf/hfss/, Ansoft Corporation HFSS, USA.